Research Article

Comparison of Theoretical & Experimental studies of 2-oxo-4-phenyl quinoline

D. Mageswari and G. Selvi*

Department of Chemistry, PSGR Krishnammal College for Women, Peelamedu, Coimbatore, Tamilnadu, India-641004

Abstract

2-oxo-4-phenyl-quinoline was synthesized from ethyl benzoyl acetate. The compounds were characterized by IR, ^{1}H NMR, ^{13}C NMR spectra and Single-crystal X-ray diffraction studies. The theoretical studies were predicted by utilizing DFT/B3LYP and HF with 6-31G (d, p) as basis set in Gaussian 09. Natural Bond Orbital (NBO) analysis is also used to explain the molecular stability. NMR chemical shifts are calculated by using GIAO shielding tensors. The experimental results of XRD, IR, ^{1}H NMR and ^{13}C NMR are in very good agreement with the theoretical studies. In addition, molecular electrostatic potential (MEP) and frontier molecular orbital analysis, Fukui and local softness indices were investigated using theoretical calculations. Based on the theoretical and experimental results, the reactions conditions and the reactivity towards the electrophilic & nucleophilic attacks were predicted.

Keywords: 2-oxo-4-phenyl- quinolone, XRD, NMR, NBO, Density functional theory, Fukui function

***Correspondence**

Author: G. Selvi

Email: selvi_gv@rediffmail.com

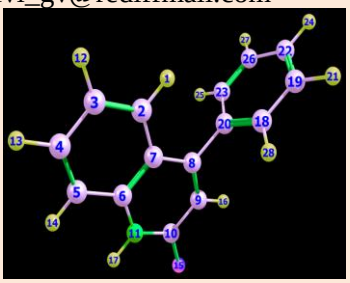

Introduction

Five or six membered heterocyclic compounds possess wide range of pharmacological activities such as anti-microbial activity [1-5], anticancer [6-8] activity, breast cancer [9], Antitubercular [10], anti-inflammatory [11], analgesic [11] and antimalarial [12] activities. 2-oxo-4-phenyl quinoline serve as a precursor for the construction for five or six membered heterocyclic compounds such as pyrano quinoline, furo quinoline, pyrrolo quinoline, naphthyridines, thieno quinoline, pyridazino quinoline, triazino quinolines etc., hence a theoretical prediction of the physical and chemical behaviour of the precursor 2-oxo-4-phenyl quinoline would be a helpful tool for the construction of desired ring fusion to the parent titled compound and their structural and spectroscopic characterization is very crucial. In the present work the crystal structure of 2-oxo-4-phenyl quinoline and IR, ^{1}H NMR, ^{13}C NMR of 2-oxo-4-phenyl quinoline are reported both theoretically and experimentally. The NBO analysis, Mulliken charges and molecular electrostatic potential, Fukui and local softness indices were also reported.

Experimental details

Thin layer chromatography (TLC) was performed using glass plates coated with silica gel. Petroleum ether and ethyl acetate was used as eluent. Spots were visualized with iodine. Purification of crude sample was carried out using chromatographic column packed with silica gel. Melting points were determined with a Labtronics digital auto melting point apparatus. IR spectra were determined as Shimadzu IR Affinity-1 instrument and the absorption frequencies quoted in reciprocal centimeters. ^{1}H NMR and ^{13}C NMR spectra were recorded on using a Bruker AV 500 MHz spectrometer using tetramethylsilane (TMS) as an internal reference and results are expressed as δ (ppm) values. For the crystal structure determination, the single-crystal of the compound $C_{15}H_{11}NO$ was used for data collection on an Ernaf Nonius CAD4-MV31 Bruker Kappa APEXII diffractometer.

2-oxo-4-phenyl quinoline were synthesized from ethyl benzoyl acetate. Benzoyl acetanilide was cyclized with H_2SO_4 gives 2-oxo-4-phenyl quinoline [13, 14]. The compounds were characterized by IR, ^{1}H NMR, ^{13}C NMR

spectra and Single-crystal X-ray diffraction studies. The white crystal was obtained at (50:50) PE: EA was attested to be 2-oxo -4-phenyl quinoline from its spectral data.

Computational details

In the present study, the HF and density functional theory (DFT/B3LYP) at the 6-31G (d, p) basis set level was adopted to calculate the optimized parameters and vibrational frequencies of 2-oxo-4-phenyl quinoline **Figure 1**. NMR chemical shifts are calculated by using GIAO shielding tensors. Natural bond orbital (NBO) calculations were performed using the NBO code. All calculations were performed using Gaussian 09 program package [15].

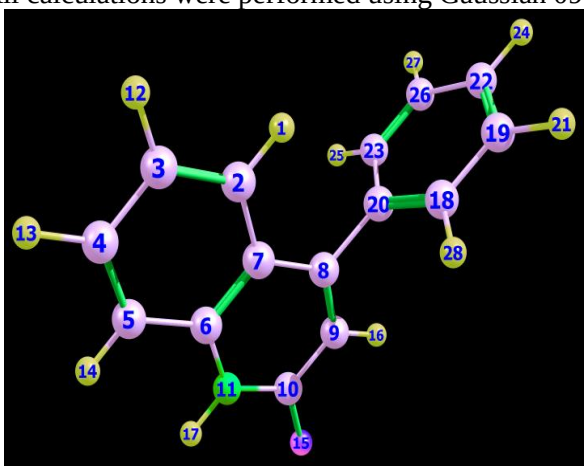

Figure 1 optimized geometry of 2-oxo-4-phenyl quinoline

Results and Discussion

IR spectral analysis

Vibrational frequency has been shown to be effective in the identification of functional groups of organic compounds as well as in studies on molecular conformations and reaction kinetics. 2-oxo-4-phenyl quinoline has 28 atoms, which undergo 78 normal modes of vibrations. The frequencies of the compound was organized in **Table 1**. The stretching vibration observed in the region around 3500-3300cm^{-1}, the band at 3265cm^{-1} in IR and at 3604cm^{-1} in B3LYP. The carbon-hydrogen stretching vibrations give rise to bands in the region 3100-3000cm^{-1} in all aromatic compounds. C-H stretching vibrations are observed at 3219, 3213, 3210, 3204, 3198, 3197, 3188, 3184, 3181cm^{-1} in B3LYP method and at 2925cm^{-1} in IR. The ring C=O stretching vibration occurs in the region 1600-1700cm^{-1}. For 4-phenyl-2-hydroxy quinoline, it is at 1659cm^{-1} in IR and 1785 cm^{-1} in B3LYP.

Table 1 IR bands and calculated (scaled) wave numbers of 2-oxo-4-phenyl- quinoline and assignments.

HF/6-31G		B3LYP/6-31G		IR υ (cm^{-1})	Assignments
υ(cm^{-1})	IR$_I$ (Å^4/amu)	υ(cm^{-1})	IR$_I$ (Å^4/amu)		
4148	**132**	**3604.779**	**41.124**	**3265**	**υN$_{11}$H$_{17}$**
3388	**11.9**	**3218.624**	**11.1067**	**2925**	**υCH**
1826	**370.8**	**1785.143**	**681.9486**	**1659**	**υC$_{10}$O$_{15}$(C=O)**
υ-stretching					

^{1}H NMR and ^{13}C NMR spectral analysis

With TMS as an internal standard, experimental spectrum data of 2-oxo-4-phenyl quinoline in $CHCl_3$ is obtained at 500MHz. B3LYP/GIAO was used to calculate the magnetic shielding of 2-oxo-4-phenyl quinoline. Relative chemical shifts were then estimated by using the corresponding TMS shielding: for ^{1}H NMR σ =30.84ppm, for ^{13}C NMR σ ($CHCl_3$) = 193.7ppm. In the ^{1}H-NMR spectrum one type of protons appears at 4.18 ppm (H-17) as a singlet (N-H). The calculated chemical shifts of ^{1}H-NMR in good correlation with the experimental observations of chemical shifts by using chloroform as a solvent. ^{13}C NMR chemical shifts in the ring for 2-oxo-4-phenyl quinoline are

>100ppm. The calculated chemical shifts of ^{13}C NMR give a good correlation with the experimental observations of ^{13}C NMR chemical shifts by using chloroform as a solvent. The calculated and experimental chemical shift values are given in **Table 2** shows a good agreement with each other. The calculated IR and chemical shifts value (**Figure 2-7** and Table 1, 2) gives a good dovetailing with the experimental observations value of 2-oxo-4-phenyl quinoline.

Table 2 The experimental and calculated ^{1}H NMR and ^{13}C NMR chemical shifts (ppm).

Assignment	**Theoretical (σ_{TMS} =30.8) $\delta_{calc} = \sigma_{TMS} - \sigma_{calc}$**		**Experimental δ_{ppm}**	**Assignment**	**Theoretical (σ_{CHCl3}=193.7) $\delta_{calc} = \sigma_{CHCl3} - \sigma_{calc}$**		**Experimental δ_{ppm}**
	σ_{calc}	δ_{calc}			σ_{calc}	δ_{calc}	
H1, H14	23.83	6.97	7.43	C10	**37.32**	**155.98**	**163.08**
H13	24.04	6.76	7.4	C8	42.36	151.34	154.04
H28	24.11	6.69	7.38	C6	49.65	144.05	137.04
H21, H24, H25, H27	24.21	6.59	**7.19**	C20	62.51	131.19	132.1
H12	24.56	6.24	7.08	C4	69.16	124.54	130.5
H16	24.98	5.82	6.66	C23	70.29	123.41	129
H17	26.19	4.61	4.18	C18	70.58	123.12	128.8
				C19, C22	72.02	121.68	128.6
				C2	72.68	121.02	126.7
				C26	73.66	120.04	124.2
				C5	75.08	118.62	122.3
				C7	79.18	114.52	120.6
				C3	80.47	113.23	119.7
				C9	92.54	101.16	106

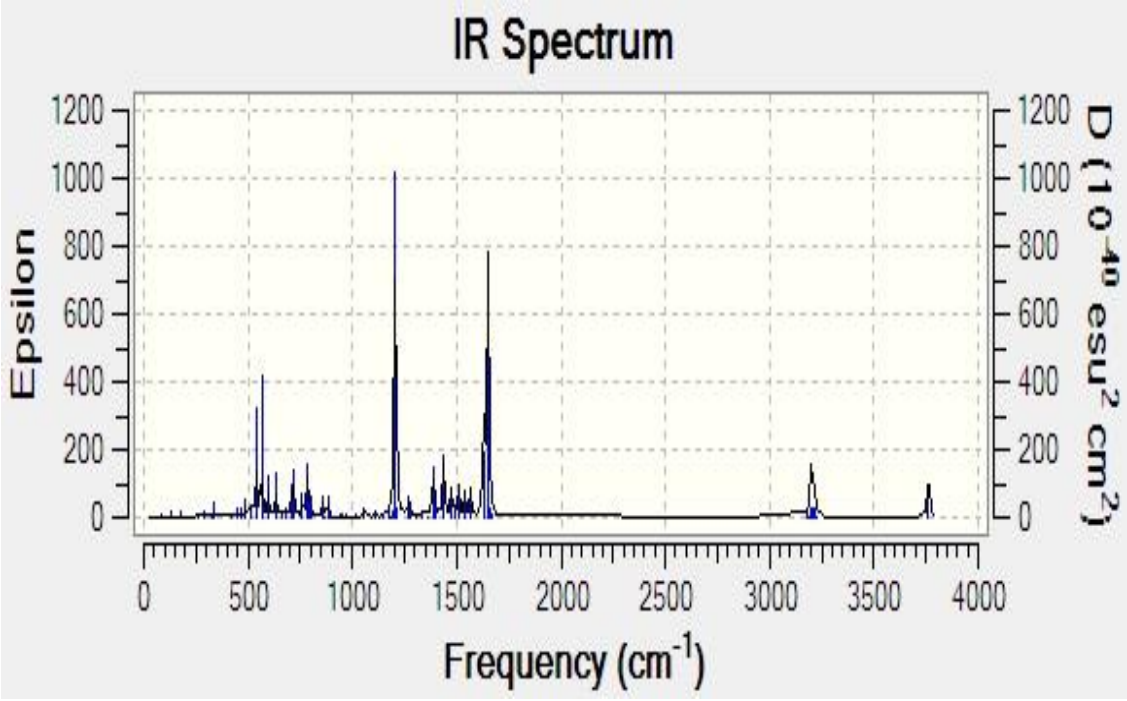

Figure 2 Theoretical IR Spectrum of 2-oxo-4-phenyl quinoline.

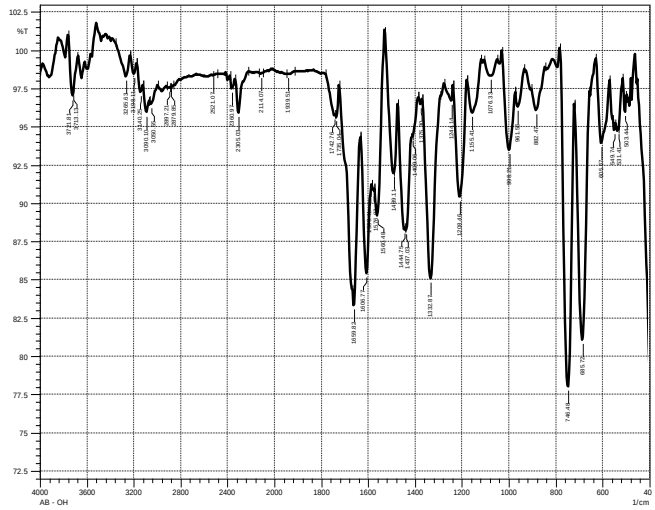

Figure 3 FT-IR Spectrum of 2-oxo-4-phenyl quinoline.

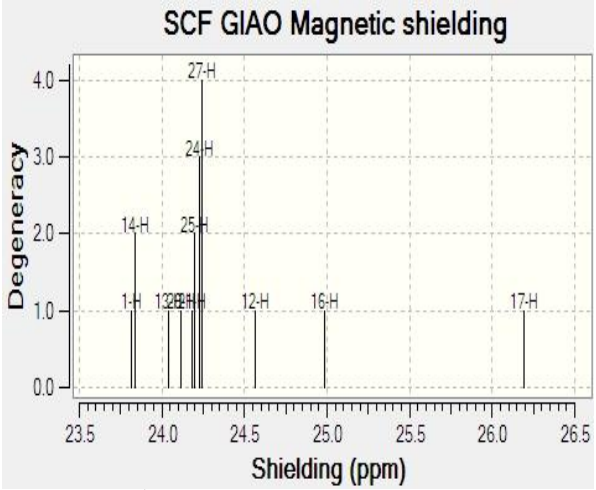

Figure 4 Theoretical [1]H NMR Spectrum of 2-oxo-4-phenyl quinoline.

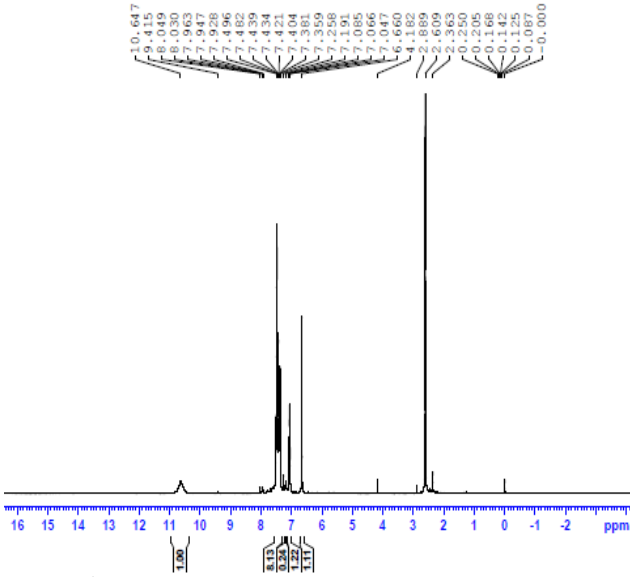

Figure 5 [1]H NMR Spectrum of 2-oxo-4-phenyl quinoline.

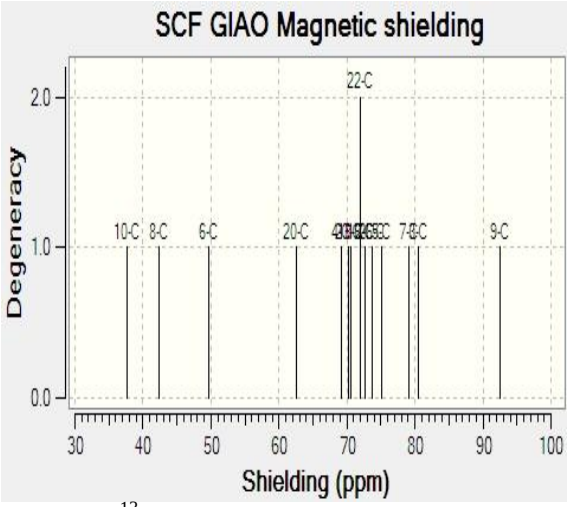

Figure 6 Theoretical ^{13}C NMR Spectrum of 2-oxo-4-phenyl quinoline.

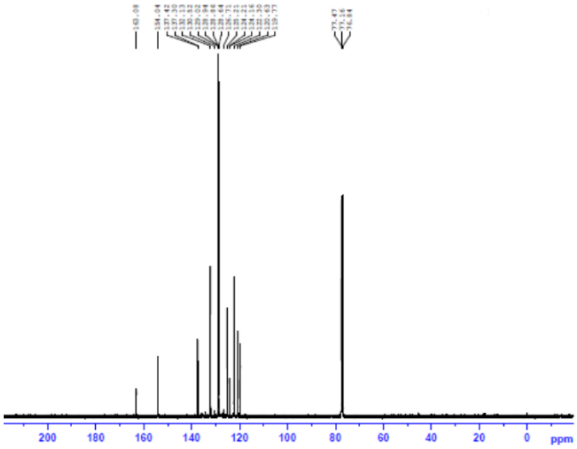

Figure 7 ^{13}C NMR Spectrum of 2-oxo-4-phenyl quinoline.

X-ray diffraction study

X-ray diffraction data was collected on an automated Ernaf Nonius CAD4-MV31 Bruker Kappa APEXII diffractometer with graphite monochromated Mo-K_α radiation, λ=0.71073Å, T=293 K. The semi empirical absorption correction of several reflections was applied which resulted in transmission factor ranging from 0.9691 to 0.9799. Crystal data and structure refinement are delineated in **Figure 8** and **Table 3**.

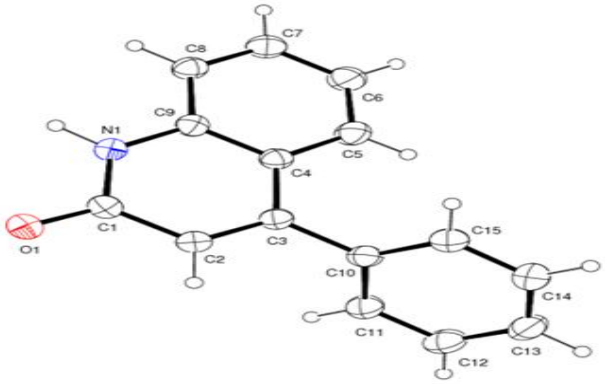

Figure 8 An ORTEP view of 2-oxo-4-phenyl quinoline with displacement ellipsoids drawn at the 30% probability level.

Table 3 Crystal data and structure refinement for 2-oxo-4-phenyl quinoline.

Empirical formula	$C_{15}H_{11}NO$
Formula Weight/a.u.	221.25
Crystal System	Orthorhombic
Space group	Pbca
a/A˚	13.9930(8)
B	7.3440(4)
C	21.6770(12)
β/˚	90.000(5)
V/ Å^3	2227.6(2)
Z	8
ρ(calc) g/cm^3	1.319
μ(Mo-K_α) mm^{-1}	0.083
Crystal size mm	0.350 x 0.350 x 0.300
T/ K	293
λ/ Å	0.71073
$\theta_{Min-Max}$/˚	2.37- 24.98
Reflections measured	26884
Independent reflections	1961
Abs. Correction	Semi-empirical
Transmission	0.969-0.979
Observed data[I > 2σ(I)]	1961
Parameters refined	159
R	0.1076
wR_2	0.1570
S	1.144

Optimized geometrical parameters

To best of our knowledge, no X-ray crystallographic data of 2-oxo-4-phenyl quinoline have yet been reported. However, the theoretical results obtained are almost comparable with the structural parameters of 2-hydroxy-4-phenyl quinoline and detailed in **Table 4**.

For 2-oxo-4-phenyl quinoline the bond length of C_1-C_2 is observed as 1.434 and1.42, 1.42Å and this length is greater than that of C_2-C_3(1.346, 1.377,1.355) because of the delocalization of electron density of C_1-C_2 due to the presence of C=O group. The greater bond length of C8-C9 (1.394, 1.417, and 1.413) is due to delocalization of electron density due to the adjacent quinoline ring. The C_7-C_8 could be assumed a double bond character due to the lesser bond length (1.352, 1.378, and 1.361). It has been reported that the bond length of C1-C2 is 1.434, C2-C3 is 1.346, C8-C9 is 1.394, and C7-C8 is 1.352. The greater bond angle N1-C1-C2-(115.7˚) is due to the presence of higher electronegative group C=O. The bond angle C2-C3-C4-119.3, C7-C8-C9-119.9, C2-C3-C4-119.3, and N1-C9-C8-119.7and N1-C9-C4-119.9 is less than 120˚ because the presences of quinoline ring. The bond angles O1-C1-C2, C3-C2-C1, C5-C4-C3, C6-C5-C4, C15-C10-C3 and C1-N1-C9 are 124.2, 122.8, 124, 121, 121, 124.2 respectively, because of the substitution of phenyl ring.

Frontier molecular orbital

The HOMO energy is directly related to the ionization potential, LUMO energy is directly related to the electron affinity. From the HOMO, LUMO calculations, the molecular electrical transport properties and also stability of the structure were predicted. According to B3LYP/6-31G (d, p) and HF calculations the energy gap is found to be 4.49889eV and 10.56680eV respectively. The atomic orbital components of the frontier molecular orbitals are shown in **Figure 9** and **Table 5**.

Table 4 Comparison of theoretical (optimized geometrical parameters (B3LYP & HF)) & experimental values of bond length and bond angle of 2-oxo-4-phenyl quinoline, atom labeling according to Figure 8.

Bond length(Å)				**Bond angle(°)**				**Dihedral angles(°)**			
	Experimental value	Theoretical value			Experimental value	Theoretical value			Experimental value	Theoretical value	
		B3LYP	HF			B3LYP	HF			B3LYP	HF
C1-O1	1.243	1.354	1.333	O1-C1-N1	120.1	118.2	119	O1-C1-C2-C3	-179	-177.80	-179.63
C1-N1	1.358	1.309	1.282	O1-C1-C2	124.2	124.8	124.7	N1-C1-C2-C3	1.3	0.00	-0.116
C1-C2	1.434	1.42	1.422	N1-C1-C2	115.7	117	116.3	C1-C2-C3-C4	-1	0.00	0.529
C2-C3	1.346	1.377	1.355	C3-C2-C1	122.8	119.1	118.8	C1-C2-C3-C10	178.6	179.981	179.981
C2-H2	0.93	1.084	1.073	C3-C2-H2	118.6	121.6	122.2	C2-C3-C4-C5	-178.3	-178.34	-178.83
C3-C4	1.44	1.44	1.44	C1-C2-H2	118.6	119.3	122.2	C10-C3-C4-C5	2.1	6.893	5.110
C3-C10	1.484	1.489	1.494	C2-C3-C4	119.3	118.2	118.4	C2-C3-C4-C9	0.8	1.638	1.279
C4-C5	1.394	1.419	1.416	C2-C3-C10	120.4	119.2	119.5	C10-C3-C4-C9	-178.7	-178.60	-178.95
C4-C9	1.395	1.433	1.406	C4-C3-C10	120.3	122.6	122.1	C9-C4-C5-C6	0.4	-0.149	-0.218
C5-C6	1.367	1.379	1.362	C5-C4-C9	118	118.5	118.8	C3-C4-C5-C6	179.5	180	180
C5-H5	0.93	1.084	1.073	C5-C4-C3	124	124	123.8	C4-C5-C6-C7	1.2	-0.842	-0.590
C6-C7	1.382	1.412	1.41	C9-C4-C3	118	117.5	117.3	C5-C6-C7-C8	-1.2	0.424	0.299
C6-H6	0.93	1.086	1.075	C6-C5-C4	121	121	120.8	C6-C7-C8-C9	-0.4	1.015	0.749
C7-C8	1.352	1.378	1.361	C6-C5-H5	119.5	119.9	119.9	C7-C8-C9-N1	-178.1	-178.14	-178.821
C7-H7	0.93	1.086	1.076	C4-C5-H5	119.5	119.1	119.3	C7-C8-C9-C4	2	-2.197	-1.671
C8-C9	1.394	1.417	1.413	C5-C6-C7	120	120.3	120	C5-C4-C9-N1	178.1	-179.18	-179.484
C8-C8	0.93	1.085	1.074	C5-C6-H6	120	119.9	120.1	C3-C4-C9-N1	-1	1.014	-1.018
C9-N1	1.367	1.386	1.362	C7-C6-H6	120	119.9	119.8	C5-C4-C9-C8	-2	0.561	0.214
C10-C15	1.376	1.405	1.392	C8-C7-C6	120.7	120.3	120.5	C3-C4-C9-C8	178.9	179.81	179.43
C10-C11	1.378	1.404	1.39	C8-C7-H7	119.7	120	120	C2-C3-C10-C15	-115.4	-124.60	-128.13
C11-C12	1.378	1.394	1.386	C6-C7-H7	119.7	119.7	119.6	C4-C3-C10-C15	64.2	52.925	83.594
C11-H11	0.93	1.086	1.075	C7-C8-C9	119.9	120.7	120.5	C2-C3-C10-C11	64.1	60.20	60.27
C12-C13	1.396	1.086	1.384	C7-C8-C8	120	121.8	121.7	C4-C3-C10-C11	-116.3	-113.39	118.334
C12-H12	0.93	1.086	1.076	C9-C8-H8	120	117.5	117.8	C15-C10-C11-C12	0.5	-0.027	0.173
C13-C14	1.361	1.396	1.386	N1-C9-C8	119.7	118	117.9	C3-C10-C11-C12	-178.9	-179.66	179.921
C13-C13	0.93	1.086	1.076	N1-C9-C4	119.9	122.8	122.8	C10-C11-C12-C13	0.6	-0.293	-0.229
C14-H15	1.375	1.394	1.384	C8-C9-C4	120.4	119.2	119.4	C11-C12-C13-C14	-0.9	0.257	0.296
C14-H14	0.93	1.086	1.076	C15-C10-C11	118.9	118.6	118.9	C12-C13-C14-C15	0.1	0.097	-0.042
C15-H15	0.93	1.086	1.076	C15-C10-C3	121	121.3	120.8	C13-C14-C15-C10	1.1	-2.369	-0.925
N1-H1A	0.92	0.971	0.947	C11-C10-C3	120.1	120.1	120.2	C11-C10-C15-C14	-1.4	-0.925	0.691
				C10-C11-C12	120.1	120.7	120.5	C3-C10-C15-C14	178.1	179.51	178.01
				C10-C11-H11	120	119.2	119.5	O1-C1-N1-C9	178.8	179.74	178.92
				C12-C11-H11	120	120.1	119.9	C2-C1-N1-C9	-1.6	0.135	0.54
				C13-C12-C11	120.6	120.2	120.2	C8-C9-N1-C1	-178.4	-178.2	-179.44
				C13-C12-H12	119.7	120.1	120.1	C4-C9-N1-C1	1.5	1.39	1.62
				C11-C12-H12	119.7	119.7	119.7				
				C14-C13-C12	119.4	120.2	119.7				
				C14-C13-H13	120.3	120.2	120.1				
				C12-C13-H13	120.3	120.2	120.2				
				C13-C14-C15	120.6	120.3	120.2				
				C13-C14-H14	119.7	120.1	120.1				
				C15-C14-H14	119.7	119.6	119.7				
				C14-C15-C10	120.5	120.6	120.5				
				C14-C15-H15	119.8	119.9	119.9				
				C10-C15-H15	119.8	119.5	119.6				
				C1-N1-C9	124.2	123.2	123.6				
				C1-N1-H1A	117.9	118.1	118.3				
				C9-N1-H1A	117.8	118.3	118.1				

The lower value of the E_{LUMO} = -1.45119 eV indicates the easier of the acceptance of electrons. The calculations indicate that the 2-oxo-4-phenyl quinoline has a low energy gap (4.49889eV) and also has low hardness value (2.24946eV) and has high softness value (0.44455 eV). From that the molecule avoids the resistance towards the deformation or polarization of the electron cloud of the atoms, ions or molecules under small perturbation of chemical reaction. So the stability of the molecule is less, so it is more reactive.

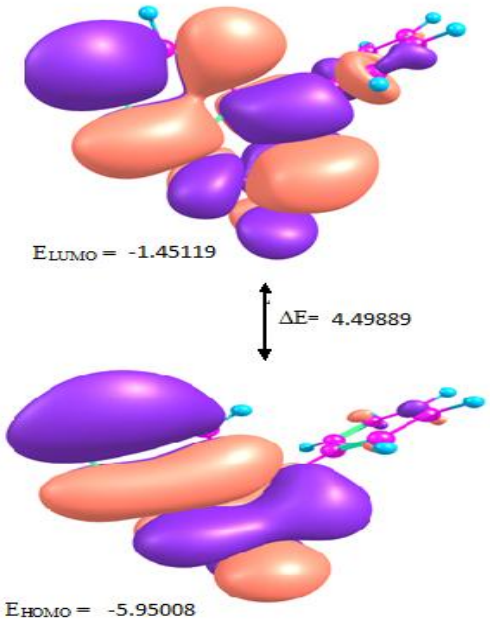

Figure 9 Atomic orpital composition of 2-oxo-4-phenyl quinoline.

Table 5 Quantum chemical parameters of 2-oxo-4-phenyl quinoline

Molecular properties	B3LYP/6-31G(d,p)	HF/6-31G(d,p)
Energy cap ΔE(eV)	4.49889	10.56680
Ionization energy I= - E_{HOMO} (eV)	5.95008	8.17790
Electron affinity A=-E_{LUMO} (eV)	1.45119	-2.43271
global hardness η(eV)	2.24946	5.30531
global softness σ(eV)	0.44455	0.18849
Electro negativity χ (eV)	3.70064	2.8726
Electronic chemical potential, μ(eV)	-3.70064	-2.8726
The global electrophilicity index, ω	3.04401	0.77770
Dipole moment	4.1476	4.7331
$\omega = \mu^2 / 2\eta$		

Mulliken charges

Mulliken charges are calculated by determining the electron population of each atom as defined in the basic functions B3LYP/6-31G (d, p). The charge distribution calculated by the Natural bond orbital (NBO) and Mulliken methods of 2-oxo-4-phenyl quinoline are reported in **Table 6**.

From Mulliken charges computation, the carbon atom C10 (0.62786) has high positive charge with compared all other carbon atoms, due to it is adjacent between two electronegative atom N&O. C10 (0.62786) behaves as acceptor atom it sustain nucleophilic reaction. C9 (-0.23418), N11 (-0.70708) and O15 (-0.55096) perform as donor atoms, it endure electrophilic reaction. We have observed changes in the charge distribution by changing different basis set are arranged in Table 6. The results were displayed in graphical form in **Figure 10**.

Table 6 The charge distribution calculated by the Natural bond orbital (NBO) and Mulliken methods of 2-oxo-4-phenyl quinoline

Atoms	Natural charges	Atomic charges M06/6-31G (Mulliken)	HF/6-31G	B3LYP/6-31G
9C	**-0.29368**	**-0.234183**	**-0.291717**	**-0.197574**
10C	**0.64139**	**0.627859**	**0.810718**	**0.595903**
11N	**-0.60307**	**-0.707075**	**-0.859246**	**-0.668729**
15O	**-0.61539**	**-0.550962**	**-0.623509**	**-0.528861**

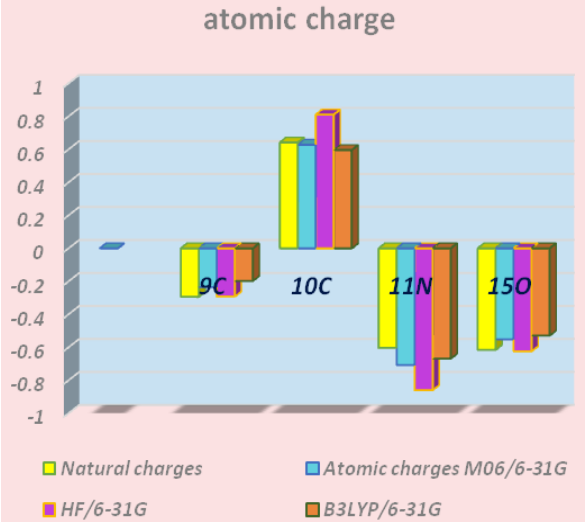

Figure 10 Comparison of different methods for calculated Mulliken charges of 2-oxo -4-phenyl quinoline.

Fukui and local softness indices

The Local reactivity has been analysed by means of Fukui indices (FI) which are indicates the reactive centers within the molecule and nucleophilic and electrophilic behaviour of the molecule. Fukui indices were widely used as descriptors of site selectivity for the soft–soft reactions. The condensed Fukui functions and condensed local softness indices is used to distinguish each part of the molecule on the basis of its distinct chemical behavior due to the different substituent functional groups. Fukui function inferred that for nucleophilic attack, the most reactive sites of 2-oxo-4-phenyl quinoline is on the carbon atom C10 of the phenyl ring; for electrophilic attack, the most reactive sites of 2-oxo-4-phenyl quinoline is on the C9, N11, and O15(**Table 7**). So 2-oxo-4-phenyl quinoline was more diligent.

Table 7 Fukui and local softness indices for nucleophilic and electrophilic attacks calculated from Mulliken atomic charge.

atoms	q_n	q_{n+1}	q_{n-1}	fk	fk+	fk-	sk+	sk-
9C	**-0.197573**	**-0.144389**	**-0.23598**	**0.0457955**	**0.053184**	**0.038407**	**0.023643**	**0.017074**
10C	**0.595903**	**0.619724**	**0.554818**	**0.032453**	**0.023821**	**0.041085**	**0.01059**	**0.018264**
11N	**-0.668729**	**-0.630924**	**-0.676687**	**0.0228815**	**0.037805**	**0.007958**	**0.016806**	**0.003538**
15O	**-0.528862**	**-0.383179**	**-0.63781**	**0.1273155**	**0.145683**	**0.108948**	**0.064764**	**0.048433**

Molecular electrostatic potential (MEP)

To predict reactive sites for electrophilic and nucleophilic attack for 2-oxo-4-phenyl quinoline, MEP was calculated at the B3LYP/6-31G (d, p) optimized geometry. MEP is related to molecular size, shape as well as positive, negative and neutral electrostatic potential regions in terms of colour grading and is very useful in research of molecular structure with its physicochemical property relationship. The colour code of these map is in the range between -0.03 a.u (deepest blue) and 0.03 a.u (deepest red) in our molecule. The negative (red and yellow- N11, O15 and C9) regions of MEP was allied with electrophilic reactivity and (green) the positive region was coupled with nucleophilic reactivity. The C=O group is perceived as electrophilic. (**Figure 11**).

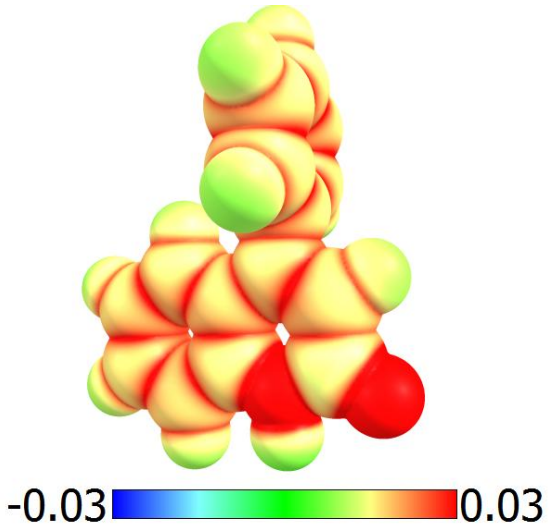

Figure 11 MEP plot of 2-oxo-4-phenyl quinoline

NBO analysis

The natural bond orbitals (NBO) calculations were performed using Gaussian 09 package at the DFT/B3LYP level. The stability of the molecule arising from hyper-conjugative interaction and charge delocalisation has been analysed using NBO analysis are reported in **Table 8**.

Table 8 Second order perturbation theory analysis of Fock matrix in NBO basis corresponding to the intra bonds of 2-oxo-4-phenyl quinoline.

Donor(i)	Type	ED/e	Acceptor(j)	Type	ED/e	E(2)[a] kJ/mol	E(i)-E(j)[b] a.u.	F(i,j)[c] a.u.
C2-C3	**π**	**1.69899**	**C4-C5**	**π***	**0.31857**	**21.79**	**0.28**	**0.063**
	π	**-**	**C6-C7**	**π***	**0.45112**	**16.66**	**0.27**	**0.039**
C4-C5	**π**	**1.71144**	**C2-C3**	**π***	**0.30260**	**16.29**	**0.29**	**0.062**
-	**π**	**-**	**C6-C7**	**π***	**0.45112**	**21.49**	**0.28**	**0.072**
C6-C7	**π**	**1.57651**	**C4-C5**	**π***	**0.31857**	**15.92**	**0.28**	**0.061**
-	**π**	**-**	**C2-C3**	**π***	**0.30260**	**20.23**	**0.29**	**0.070**
-	π	-	C6-C7	π*	0.45112	1.10	0.28	0.016
-	π	-	C8-C9	π*	0.15364	15.53	0.30	0.065
C10-O15	π	1.97992	C8-C9	π*	0.15364	5.36	0.39	0.042
-	π	-	C10-O15	π*	0.34371	1.14	0.37	0.020
C8-C9	π	1.81898	C20-C23	π*	0.35026	0.99	0.76	0.027
	π	**-**	**C6-C7**	**π***	**0.45112**	**10.91**	**0.29**	**0.054**
-	**π**	**-**	**C10-O15**	**π***	**0.34371**	**21.95**	**0.29**	**0.075**
-	π	-	C18-C20	π*	0.02348	2.80	0.84	0.045
-	π	-	C20-C23	π*	0.02439	2.80	0.84	0.045
C18-C20	π	1.66245	C8-C9	π*	0.02076	2.53	0.88	0.046
-	**π**	**-**	**C18-C19**	**π***	**0.32670**	**19.82**	**0.28**	**0.067**
-	**π**	**-**	**C22-C26**	**π***	**0.32960**	**20.45**	**0.28**	**0.068**
C19-C22	**π**	**1.66252**	**C22-C26**	**π***	**0.32960**	**20.15**	**0.28**	**0.067**
C23-C26	**π**	**1.65948**	**C20-C23**	**π***	**0.35026**	**20.48**	**0.28**	**0.068**
-	**π**	**-**	**C18-C19**	**π***	**0.32670**	**20.44**	**0.28**	**0.068**
LP N11	π	1.89891	C-6	π*	0.00170	2.24	2.05	0.067
-	π	-	C-10	π*	0.00354	1.19	2.28	0.052
-	**π**	**-**	**C6-C7**	**π***	**0.45112**	**43.99**	**0.28**	**0.102**

-	**π**	**-**	**C10-O15**	**π***	**0.34371**	**54.02**	**0.29**	**0.112**
LP O15	σ	1.97721	C-10	**π***	0.01681	15.16	1.47	0.134
-	**σ**	**-**	**N11-C10**	**σ***	**0.08734**	**28.69**	**0.66**	**0.125**
-	σ	-	C9-C10	σ*	0.05670	18.69	0.70	0.104

These interactions are observed as an increase in electron density (ED) in N-C, C-O and C-C anti bonding orbital that weakens the respective bond. In this present work, the π electron delocalization is maximum around C2-C3, C4-C5, C6-C7, C8-C9, C18-C20, C19-C22, C23-C26 distributed to π* antibonding of C6-C7, C2-C3, C4-C5, C10-O15, C23-C26, C18-C20 and C19-C22 with a stabilization energy and electron density of about 21.19, 21.79, 20.23, 21.95, 20.45, 20.95, 20.48 kJ/mol and 0.45112, 0.31857, 0.30260, 0.34371, 0.32960, 0.35026, 0.35026 respectively as shown in Table 8. The most important interaction is LP N11→ π*(C10-O15), π*(C6-C7) and with the stabilization energy and electron density of about 54.02, 43.99 kJ/mol and 0.45112, 0.343701 respectively. The most important interaction is LP O15 → σ*(N11-C10)) and with the stabilization energy and electron density was 28.69 kJ/mol and 0.08734.

There occurs a strong intermolecular hyper conjugative interaction of C6-C7 from N-11of n1 (N-11) → π*(C6-C7) which increases ED (0.45112e) that weakens the respective bonds C6-C7 leading to stabilization of 43.99 kJ/mol. There occurs a strong intermolecular hyper conjugative interaction of C10-O15 from N-11 of n1(N-11) → π*(C10-O15) which increases ED(0.34371) that weakens the respective bonds C10-O15 leading to stabilization of 54.02kJ/mol. These interactions are observed as an increase in electron density (ED) in C-C, and C-O antibonding orbitals that weakens the respective bond.

Conclusions

The crystal structure of the compound 2-oxo-4-phenyl quinoline has been characterized by single crystal X-ray diffraction method and spectroscopic technique. The calculated IR, ^{1}H NMR and ^{13}C NMR results are in good consensus with experimental data. The reactive sites of 2-oxo-4-phenyl quinoline were predicted by Mulliken atomic charges, NBO analysis, and molecular electrostatic potential. Molecular electrostatic potential was harmonized with Mulliken atomic charges of 2-oxo-4-phenyl quinoline. The condensed Fukui function also reinforced with NBO results. From the detailed investigation of 2-oxo-4-phenyl quinoline, we set new strategy of reaction conditions and modified and simple reaction pathways of several heterocyclic compounds were predicted easily. 2-oxo-4-phenyl quinoline are the precursor of several quinoline compounds such as pyrano quinoline, furo quinoline, pyrrolo quinoline, naphthyridines, thieno quinoline, pyridazino quinoline, triazino quinoline.

References

[1] Mohamed El Faydy , Naoufal Dahaief , Mohamed Rbaa , Khadija Ounine , Brahim Lakhrissi, J. Mater. Environ. Sci, 2016, 7 (1), p356-361.

[2] Jyotindra B. Mahyavanshi, Maharshi B. Shukla, Kokila A. Parmar and Jayesh P. Jadhav Der Pharma Chemica, 2015, 7(11), p156-161.

[3] N.C. Desai, Amit M. Dodiya, Arabian Journal of Chemistry, 2014, 7(6), p906–913

[4] Sahar Balkat Al-juboorya and Ammar A. Razzak Mahmood Kubbab, Der Pharma Chemica 2016, 8(4) p63-66.

[5] Obaid Afzal, Suresh Kumar, Md Rafi Haider, Md Rahmat Ali, Rajiv Kumar, Manu Jaggi, Sandhya Bawa, Euro J Med Chem, 2015, p871–910.

[6] K.Ilango, P.Valentina, K.Subhakar and MK.Kathiravan. Design, Synthesis and Biological Screening of 2, 4-Disubstituted Quinolines, Austin J Anal Pharm Chem. 2015, 2(4), 1048.

[7] Yadagiri Thigulla, Mahesh Akula, Prakruti Trivedi, Balaram Ghosh, Mukund Jha and Anupam Bhattacharya , *Org. Biomol. Chem.*, 2016, 14(3), 876-883.

[8] P.-Y. Chung, J. C.-O. Tang, C.-H. Cheng, Z.-X. Bian, W.-Y. Wong, K.-H. Lam and C.-H. Chui *SpringerPlus* 2016 5, p271.

[9] Mostafa M. Ghorab, Mansour S. Alsaid, Acta Pharm., 2015, 65, p271–283.

[10] Mahesh Akula P. Yogeeswari, D. Sriram, Mukund Jha and Anupam Bhattacharya *RSC Adv.*, 2016, 6(52), p46073-46080.

[11] Sujeet Kumar Gupta and Ashutosh Mishra Anti-Inflammatory & Anti-Allergy Agents in Med Chem, 2016, 15(3).

[12] Rahul B. Shah , Nikunj N. Valand , Pinkesh G. Sutariya , Shobhana K. Menon Journal of Inclusion Phenomena and Macrocyclic Chemistry, 2016, 84(1), p173-178.

[13] Reynold C. Fuson, Donald M. Burness ‘‘A new synthesis of 2-aryl-4-hydroxy quinolines”. 1946, 68, p1270-1272.

[14] Robert C. Elderfield, Walter J. Gensler, Thomas H. Bembry, Chester B.Kremer, James D.Head, Frederick Brody and Roger Frohardt, ‘‘Synthesis of 2-phenyl-4-chloro quinolines”, 1946, 68, p 1272-1276.

[15] M.J.Frisch,G.W.Trucks,H.B.Schlegel,G.E.Scuseria,M.A. Robb, J.R. Cheeseman,G. Scalmani, V. Barone, B. Mennucci, G.A. Petersson, H. Nakatsuji, M. Caricato,X. Li, H.P.Hratchian,A.F. Izmaylov, J. Bloino, G. Zheng, J.L. Sonneberg, M. Hada,M. Ehara, K. Toyota, R. Fukuda,J. Hasegawa, M. Ishida, T. Nakajima, Y. Honda,O. Kitao, H. Nakai, T. Vreven,J.A. Montgomery,J.E. Peralta, F. Ogliaro, M.Bearpark, J.J. Heyd, E. Brothers, K.N. Kudin, V.N. Staroverov,T. Keith, R.Kobayashi, J. Normand, K. Raghavachari, A. Rendell, J.C. Knox, J.B. Cross, V.Bakken, C. Adamo, J. Jaramillo, R. Gomperts, R.E. Stratmann, O. Yazyev, A.J.Austin, R. Cammi, C. Pomelli, J.W. Ochterski, R.L. Martin, K. Morokuma, V.G.Zakrzewski, G.A. Voth, P. Salvador, J.J. Dannenberg, S. Dapprich, A.D. Daniels, O.Farkas, J.B. Foresman, J.V. Ortiz, J. Cioslowski, D.J. Fox, Gaussian09, Revision B.01, Gaussian Inc., Wallingford, CT, 2010.

Publication History
Received 15th Apr 2016
Accepted 10th May 2016
Online 05th Oct 2016